

Degradation of Acid Blue 113 in aqueous solutions by the electrochemical advanced oxidation in the presence of persulfate

Ali Reza Rahmani^a, Amir Shabanloo^a, Mehdi Fazlzadeh^b, Yousef Poureshgh^{a,*}, Hadi Rezaeivahidian^c

^aDepartment of Environmental Health Engineering, School of Public Health, Hamadan University of Medical Sciences, Hamadan, Iran, Tel. +989181317314, email: rahmani@umsha.ac.ir (A.R. Rahmani), Tel. +989183786151, email: Shabanlo_a@yahoo.com (A. Shabanloo), Tel. +989148092356, Fax +984533512004, email: yusef.poureshgh@gmail.com (Y. Poureshgh)

^bDepartment of Environmental Health Engineering, School of Public Health, Ardabil University of Medical Sciences, Ardabil, Iran Tel. +989148090705, email: m.fazlzadeh@gmail.com

^cDepartment of Chemistry and Chemical Engineering, Malek Ashtar University of Technology, Tehran, Iran Tel. +989123068986, email: h.Rezaeivahidian@gmail.com

Received 21 September 2015; Accepted 10 June 2016

ABSTRACT

Azo dyes can lead to a number of problems in the environment due to the presence of benzene rings in their structures. Therefore, the removal of these pollutants is necessary before being discharged directly into the environment. The aim of the present study was to investigate the efficiency of Persulfate ($S_2O_8^{2-}$) in the degradation of Acid Blue 113 (AB113) by electrically generated iron from the iron anode electrode. In the study, an electrolytic batch reactor equipped with four electrodes and a direct current power supply was used to degrade AB113. pH changes throughout the reaction, synergic effects of related parameters in the system and analysis of UV-Vis spectrum of AB113 were investigated under optimum conditions. The results showed that initial pH of the solution, initial concentration of $S_2O_8^{2-}$ and current density had a significant influence on the decolorization efficiency. The dye degradation was higher under acidic conditions and decreased by pH increase. After 2 min of reaction time at pH 3, 5, 7, 9 and 11, decolorization, efficiencies of 99, 66, 0, 0 and 13.5% were achieved, respectively. An increase in current density (0.625 – 15.625 A m^{-2}) increased dye removal. $S_2O_8^{2-}$ individually removed 17% of the dye after 2 min. In addition, under the same conditions, the electrochemical process individually showed 31% efficiency. However, electro/persulfate achieved decolorization efficiency by 99.8%. Thus, the use of this process can be a promising method for the operators of industrial wastewater treatment plants.

Keywords: Sulfate radical; Electro/persulfate; Activation; Iron electrode; Acid Blue 113

1. Introduction

Rapid development of textile industry and extensive use of synthetic dyes in recent decades have introduced various dyes as a major source of water pollution [1,2]. Synthetic dyes are also widely used in various industries such as leather, cosmetics, printing inks, foodstuffs, paper and plastics and dyestuff production [3]. Annually, over 7×10^5 tons of dyestuff are produced worldwide. Almost 10–15% of the total

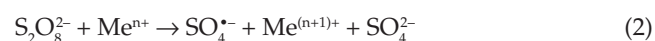
amount of the dyes used is found in the effluents disposed from such industries into the environment without any pre-treatment [3]. Moreover, azo dyes comprise 70% of all produced dyes in the world; these dyes, due to the presence of azo groups ($-N=N-$) and aromatic rings in their structure, are slowly degrade in the environment; besides, they have toxic, mutagenic, carcinogenic characteristics and impose aesthetic problems while being discharged into water resources [4,5].

Adsorption onto activated carbon, sedimentation, photo-degradation and biodegradation, coagulation and electrocoagulation are common methods, which have been

*Corresponding author.

used successfully for the treatment of colored wastewaters. Adsorption onto activated carbon is an expensive and time-consuming method, which consequently does not yield a desirable and proper efficiency. Also, oxidation by chlorine compounds produces harmful chlorinated disinfection byproducts and flotation and coagulation only transform pollutants from liquid into solid phase [3]. In recent decades, the use of advanced oxidation processes (AOPs), as acceptable and efficient method, has attracted the attention of a huge number of researchers and plant operators.

Among these, hydrogen peroxide and ozone have been evaluated as in situ or ex situ, but their application has been limited by factors including short life spans, low water solubility and costly storage and transportation [6,7]. In the last few years, $S_2O_8^{2-}$ with an oxidation potential of 2.01 V has been introduced. It is capable of oxidizing toxic organic compounds and refractory organics. Some advantages of this compound are as follows: cost effectiveness, non-selective oxidation of organic compounds, high stability of generated radicals under different conditions, high solubility and easy transportation and storage (because of its solid phase) [8,9]. Nonetheless, many studies have claimed that its reaction with organic compounds is generally slow at normal temperature. Therefore, activation of $S_2O_8^{2-}$ has been proposed as a way for accelerating the degradation process. Generally, heat, UV or transition metals (Me^{2+}) can activate persulfate. The end product of the activation process is sulfate radical ($SO_4^{\cdot-}$) with a oxidation potential of 2.6 V. Eqs. (1) and (2) show the thermal and chemical activation of $S_2O_8^{2-}$ [6,10–14]:



Among transition metals, ferrous ions (Fe^{2+}) has been widely used to activate $S_2O_8^{2-}$ (Eq. (3)). However, there are some drawbacks with the application of Fe^{2+} , which include requirement a high concentration of Fe^{2+} , generation of a large amount of iron sludge, conversion of Fe^{2+} into ferric ions (Fe^{3+}) after reaction with $S_2O_8^{2-}$ and consumption of $SO_4^{\cdot-}$ radicals at high concentrations [7,15–17].



Rong Xu et al. [18], who studied the efficiency of persulfate activated by Fe^{2+} for degradation of Orange G, reported that under optimum conditions for the removal of 99% of the dye at concentration of 0.1 mM and contact time 30 min, was 4 mM $S_2O_8^{2-}$ and Fe^{2+} at pH 3.5.

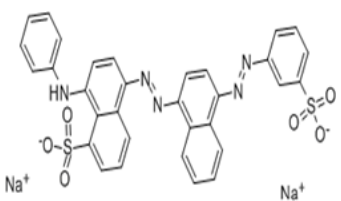
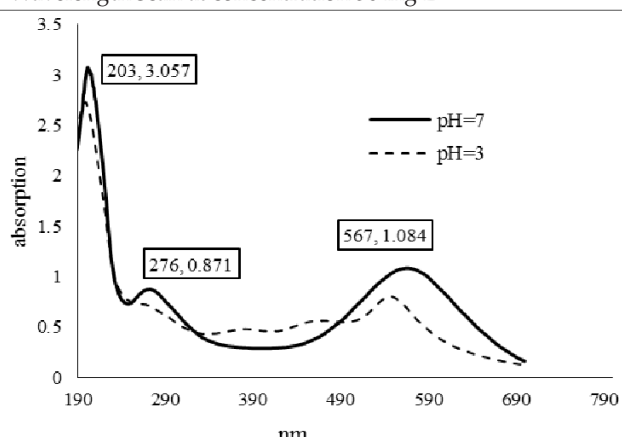
Young Oh et al. [7] used zero valent iron (Fe^0), as a source of Fe^{2+} generation, for the activation of $S_2O_8^{2-}$ in order to degrade 2,4-dinitrotoluene at pH ranging 3–3.2 and found that Fe^0 activated $S_2O_8^{2-}$ more efficiently and resulted in more pollutant removal; also, they reported that $S_2O_8^{2-}$ separately had a negligible role in pollutant removal. Another study by Jie Wu et al. [19], in which electro/ Fe^{2+} /peroxydisulfate process was used to degrade Acid Orange 7, found that the combination of electrochemical with $S_2O_8^{2-}/Fe^{2+}$ processes enhanced the decolorization efficiency. Ferrous ion was added externally to the reactor. Ti/ RuO_2 - IrO_2 and stainless steel were used as anode and cathode, respectively. Considering the specific advantages of the electrochemical process to remove organic compounds, especially colored compounds, as well as high decolorization efficiency, the main purpose of the present study was the activation of $S_2O_8^{2-}$ using electrochemically generated iron via the iron anode electrode. Furthermore, the effects of various parameters including pH, current density, $S_2O_8^{2-}$ concentration and initial dye concentration on decolorization effectiveness were studied. In addition, pH changes throughout the experiments, the synergetic effect of various parameters and UV-vis spectral changes with time under optimum conditions were investigated.

2. Material and methods

2.1. Chemicals

Acid Blue 113 was purchased from Alvan Sabet Co., Hamadan, Iran. Sodium hydroxide, sulfuric acid, sodium and potassium persulfate were purchased from Merck (Germany). Direct current power supply (PS-405), digital pH meter and spectrophotometer (DR5000, HACH) were used. Characteristics of Acid Blue 113 have been given in Table 1.

Table 1
Characteristics of Acid Blue 113

Name	Acid Blue 113	Wavelength scan at concentration 50 mg L ⁻¹
Molecular structure		
Molecular formula	$C_{32}H_{21}N_5Na_2O_6S_2$	
Molecular weight	681/85 g mol ⁻¹	
Alternative name	Acid Fast Blue 5R	

2.2. Experimental setup

The study was performed in water and wastewater laboratory of Hamadan University of Medical Sciences in winter 2013. The experiments were performed in a 1250 mL electrolytic batch reactor (plexiglass) containing 1000 mL of each sample. Four iron electrodes (2 anodes and 2 cathodes) were placed vertically in the reactor at a distance of 20 mm. Dimensions of the electrodes were same as $2 \times 20 \times 200 \text{ mm}^3$. All these four electrodes were connected to a direct current power supply by wire links. The schematic of the experimental setup employed in the present study is shown in Fig. 1. NaOH (1N) and H_2SO_4 (1N) were used to adjust solution pH. 100 mg l^{-1} of Na_2SO_4 was added to all experiments in order to enhance the ionic strength of the solutions. Desired concentrations of the dye ($100\text{--}1000 \text{ mg l}^{-1}$) were prepared from stock dilution (1 g in 1000 ml of distilled water). Also, appropriate contents of $\text{S}_2\text{O}_8^{2-}$ ($25\text{--}1000 \text{ mg l}^{-1}$) were added into the reactor. The range of current density was adjusted at $0.625\text{--}16.625 \text{ A m}^{-2}$.

The theoretical amount of metal dissolved from the anode electrode in electrochemical process can be calculated according to Eq. (4):

$$M_{\text{theo}} = \frac{MIt}{nF} \quad (4)$$

where M_{theo} is the mass of the metal dissolved (g), I is the current (A), t is the time of EC process (s), M is the molecular weight of the metal (g mol^{-1}), n is the number of electrons involved in the redox reaction (for the Iron $n = 2$) and F is the faraday constant ($96,487 \text{ C mol}^{-1}$ of electron).

Also, current density is calculated by Eq. (5).

$$CD = \frac{I}{S} \quad (5)$$

where CD is current density (A m^{-2}), I is current (A), and S is the surface area of anode electrode (m^2).

All experiments were carried out under mixing (200 rpm) to ensure good dispersion of the solution. and reaction time for each experiment was 30 min. All samples were withdrawn in the predetermined time intervals (0–30 min) during

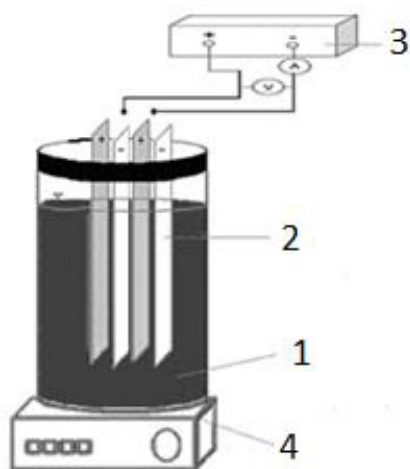


Fig. 1. Schematic of the experimental setup employed in the present study (1. Electrochemical cell 2. cathode and anode electrodes 3. Direct current power supply 4. magnetic stirrer).

each reaction. A volume of 50 mL was used for each analysis. Before reading the samples, they were centrifuged for 1 min at 2500 rpm in order to remove any remaining sludge.

2.3. Determination of Acid Blue 113

In order to determine the residual concentrations of Acid Blue 113, the wavelength of 567 nm was used. To select the wavelength, an appropriate amount of the dye was prepared at neutral pH. Color changes were determined by a UV–Vis spectrophotometer (DR5000) and in quartz cuvettes at a wavelength range of 190–700 nm. The absorption peak occurred at a wavelength of 567 nm. To determine how pH value influences this wavelength range, all these steps were repeated for the samples with $\text{pH} < 3$. Wavelength scans showed that any change in pH value changed or reduced the peak values. Thus, the pH of all samples was fixed at 7 before reading. The results of the scans have been shown in Table 1. To calculate the amount of absorbance as concentration in mg l^{-1} , a standard curve was used. Variation of pH and current intensity (as an indicator for describing the amount of EC) were monitored during sampling. The wavelength scan was done in the range of 190–700 nm in order to determine the changes occurring in dye structure under optimum conditions. Quartz cell was used for the purpose.

3. Results

3.1. Effect of initial pH on degradation effectiveness

The effects of pH have been shown in Fig. 2. As can be seen from the figure, the highest dye removal (98.2%) was achieved at pH 3 after 2 min of reaction. The efficiency decreased significantly with increasing pH. Decolorization efficiencies at pH 5, 7, 9 and 11 were 66.5, 0, 0 and 13.5%, respectively. But with increasing contact time, removal efficiency increased and achieved by $>90\%$ in all experiments. Hence, pH 3 was selected as the optimum value.

Simultaneously, pH variations of the solutions were monitored during each run. The results have been illustrated in Fig. 3. As can be seen, pH levels of the samples changed throughout the experiments.

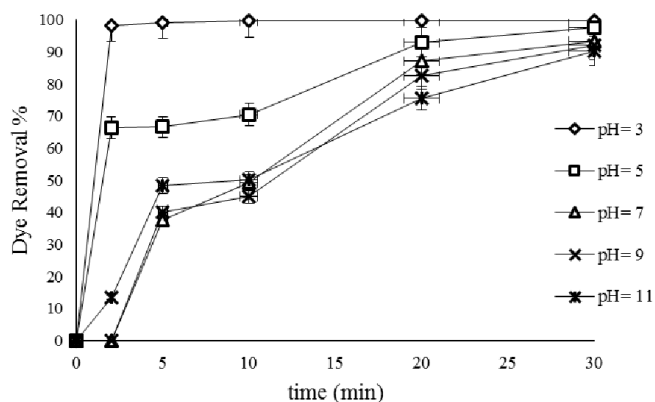


Fig. 2. Effect of pH on decolorization efficiency (dye concentration= 100 mg l^{-1} , $\text{S}_2\text{O}_8^{2-} = 150 \text{ mg l}^{-1}$, $\text{Na}_2\text{SO}_4 = 100 \text{ mg l}^{-1}$, current density = 9.375 A m^{-2}).

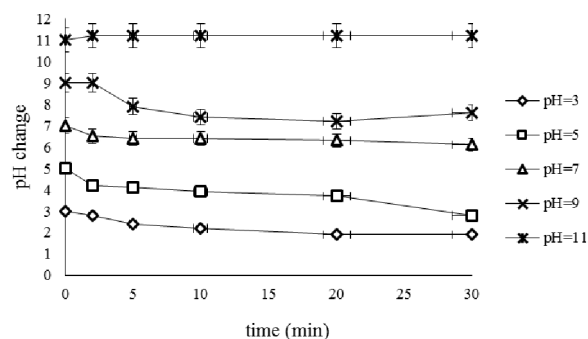


Fig. 3. pH variation during the experiments (dye concentration = 100 mg l⁻¹, S₂O₈²⁻ = 150 mg l⁻¹, Na₂SO₄ = 100 mg l⁻¹, current density = 9.375 A m⁻²).

Finally, it should be noted that the maximum pH change was observed during 5 min of reaction. As a whole there was a downward trend in pH variations. For example, final pH values dropped to 1.9 and 2.8 after 30 min with initial pH values of 3 and 5, respectively. However, it reached 11.2 at initial pH of 11 after 30 min.

3.2. Effects of current density on the degradation efficiency

Fig. 4 shows the effects of current density ranging from 0.625–16.625 A m⁻² on the efficiency. Apparently, an increase in current density from 0.625 to 9.375 A m⁻², accelerated significantly the decolorization efficiency. For instance, after 2 min at current density of 0.625, 3.125, 6.25 and 9.375 A m⁻², the efficiencies were 0, 65, 90 and 98.2%, respectively. And, no effect on decolorization effectiveness was seen when current density increased from 9.375 to 16.625 A m⁻². Also, at these current densities the decolorization efficiency remained unchanged after 5 min. Considering the results, 9.375 A m⁻² was selected as the optimum current density.

According to Eq. (2), the current is in range of 0.01–0.25 A. Therefore, the amounts of iron dissolved in the solution after 2 min according to Eq. (1) have been shown in Table 2.

3.3. Effect of S₂O₈²⁻ concentration on degradation effectiveness

The effects of variation of S₂O₈²⁻ concentrations: 25, 50, 75, 100, 150, 250, 500 and 1000 mg l⁻¹ on AB113 degradation have

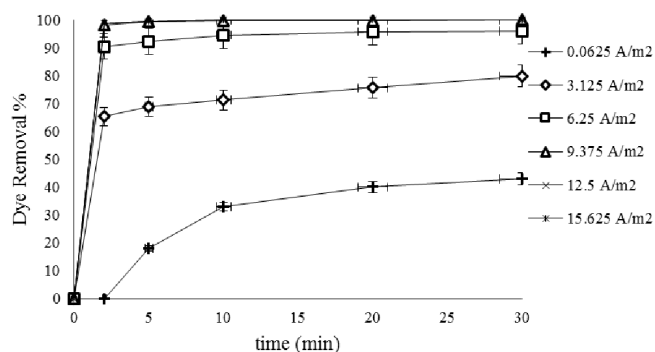


Fig. 4. Effect of current density on decolorization efficiency (dye concentration = 100 mg l⁻¹, S₂O₈²⁻ = 150 mg l⁻¹, Na₂SO₄ = 100 mg l⁻¹, pH = 3).

Table 2

Experimental and theoretical amount of iron dissolved in different current density

Current density (A m ⁻²)	0.625	3.125	6.25	9.375	12.5	15.625
Current (A)	0.01	0.05	0.1	0.15	0.2	0.25
Theoretical amount of iron dissolved (g)	0.35	1.75	3.5	5.25	6.95	8.7
Experimental amount of iron dissolved (g)	0.29	1.33	2.9	4.73	5.75	8.41

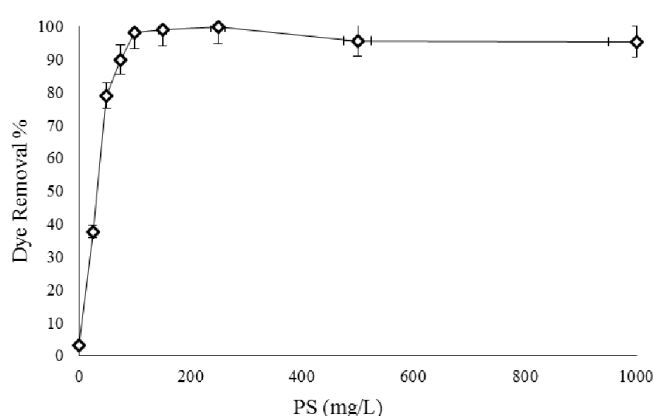


Fig. 5. Effect of S₂O₈²⁻ concentration on decolorization efficiency (contact time = 2 min, dye concentration = 100 mg l⁻¹, current density = 9.375 A m⁻², Na₂SO₄ = 100 mg l⁻¹, pH = 3).

been given in Fig. 5. The concentration of S₂O₈²⁻ plays a main role in the decolorization efficiency, as it acts as the source of SO₄⁻ generation enhancing significantly the degradation efficiencies. After 2 min at S₂O₈²⁻ concentrations of 25, 50, 75 and 100 mg l⁻¹, decolorization efficiencies achieved by 37, 79, 89 and 98.2%, respectively. With increasing concentration from 100 to 150 mg l⁻¹, only a very slight change in decolorization efficiency (99%) was observed. However, decolorization decreased by 95% after 2 min when the concentration exceeded 500 and also 1000 mg l⁻¹. Therefore, 150 mg l⁻¹ was determined as the optimum concentration.

3.4. Effect of initial concentration on decolorization efficiency

Fig. 6 shows the effects of initial AB113 concentrations of 100, 250, 500 and 1000 mg l⁻¹ on degradation rates. The results concluded that with increasing initial concentration, the degradation efficiency decreased. For example, with increasing concentration from 100 to 250 mg l⁻¹, the degradation rate decreased from 98.2 to 91%, respectively, after 2 min. But after 30 min of contact time, these efficiencies declined to 28 and 17%, respectively.

3.5. Synergistic effects of various parameters

In order to investigate the synergistic effects of various parameters: pH, Na₂SO₄, as electrolyte, and S₂O₈²⁻ on

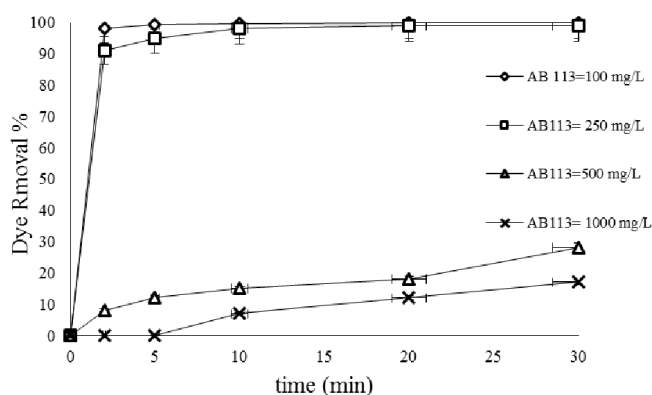


Fig. 6. Effect of dye concentration on decolorization efficiency ($S_2O_8^{2-}$ concentration = 150 mg l^{-1} , current density = 9.375 A m^{-2} , $Na_2SO_4 = 100 \text{ mg l}^{-1}$, pH = 3)

the efficiency, eight separate samples were prepared. Also, some samples were prepared to investigate the effect of $S_2O_8^{2-}$ application in the presence of electrolyte, the electrochemical process in the presence and also absence of the electrolyte, the process under its optimum conditions in the presence and absence of electrolyte.

Contact time in all samples was fixed at 20 min. The comparative results have been shown in Fig. 7. $S_2O_8^{2-}$ individually degraded the dye by 17%. Also, under the same conditions, the electrochemical process in the presence of the electrolyte and iron electrode showed individually 31% efficiency. But the efficiency increased by 99.8% in the case of the combined system, which was 51% more than the separate systems. Furthermore, the results indicated that electrolyte had a negligible effect on the efficiency. When the electrolyte concentration was zero, current density was 7.25 A m^{-2} .

3.6. Changes in UV–vis spectrum of Acid Blue 113 degradation at different times under the optimum conditions

Changes observed in UV–vis spectrum for the degradation of AB113 have been shown in Fig. 8. These results showed that the dye structure changed as the time passed.

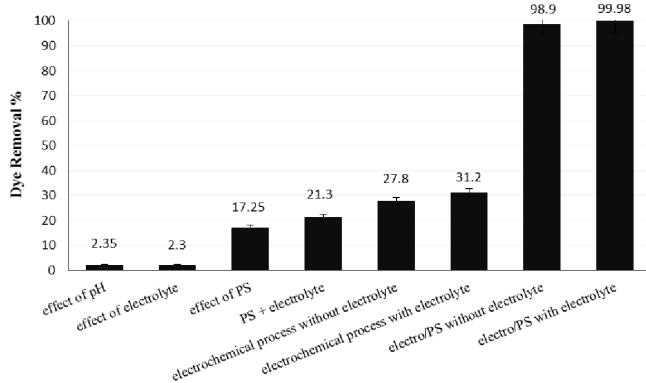


Fig. 7. Synergic effects of various parameters (pH = 3, contact time = 20 min, $S_2O_8^{2-}$ concentration = 150 mg l^{-1} , current density = 9.375 A m^{-2} , dye concentration = 100 mg l^{-1} , $Na_2SO_4 = 100 \text{ mg l}^{-1}$).

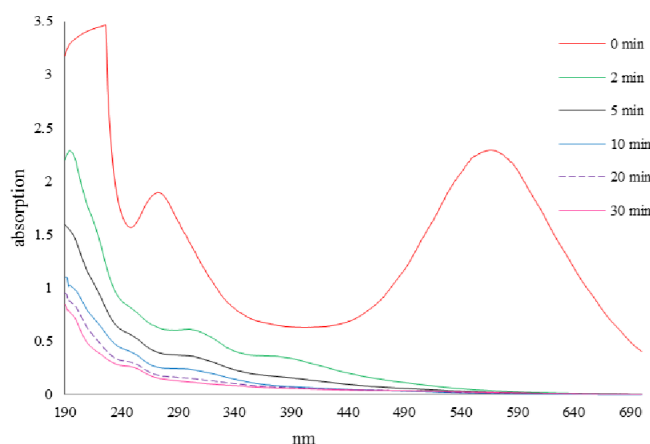


Fig. 8. UV–vis spectral changes of Acid Blue 113 (pH = 3, $S_2O_8^{2-}$ concentration = 150 mg l^{-1} , current density = 9.375 A m^{-2} , dye concentration = 100 mg l^{-1} , $Na_2SO_4 = 100 \text{ mg l}^{-1}$).

Three peaks were observed at 567, 276 and 203 nm, which all obeyed a downward trend as reaction proceeded. Among these, the peaks related to 567 nm (azo group) and 203 nm (refractory rings of AB113) showed the maximum and minimum drops, respectively.

3.7. Kinetics evaluation

In this study, to achieve this goal, Zero-order, First-order and Second-order Kinetics were studied. Table 3 shows linear forms and equations related to each one of the above kinetics.

Table 4 shows the results of kinetic coefficients of Acid Blue 113 under the effect of pH and current density in the presence of persulfate. The effect of pH values on Acid Blue 113 adsorption fitted well to the first-order kinetic model and the first-order kinetic coefficient decreased with increasing pH value, which is indicative of a decrease in the rate of the process. Moreover, the effect of current density on Acid Blue 113 adsorption fitted well to the second-order kinetic model; thus, second-order kinetic coefficient increased with increasing current density, which illustrated an increase in the rate of the reaction.

Table 3
Equations and linear forms of kinetics model

Kinetic model	Equation	Linear form
Zero-order	$r_c = \frac{dC}{dt} = k_0$	$C - C_0 = -k_0 t$
First-order	$r_c = \frac{dC}{dt} = k_1 C$	$\ln \frac{C}{C_0} = -k_1 t$
Second-order	$r_c = \frac{dC}{dt} = k_2 C^2$	$\frac{1}{C} - \frac{1}{C_0} = k_2 t$

Where r_c : the rate of conversion, C_0 : initial concentration (mg l^{-1}), C_c : equilibrium concentration in solution (mg l^{-1}), t : time, k_0 : Zero-order rate constant, k_1 : Pseudo first-order rate constant, k_2 : Pseudo second-order rate constant, R^2 : correlation coefficients.

Table 4
Kinetic coefficients of Acid Blue 113 under the effect of current density in the presence of persulfate

CD (A m ⁻²)	Zero-order		First-order		Second-order	
	k ₀	R ²	k ₁	R ²	k ₂	R ²
0.625	1.48	0.807	0.0197	0.851	0.0002	0.922
3.125	1.5	0.378	0.0348	0.534	0.001	0.813
6.25	1.6	0.262	0.0702	0.468	0.0069	0.811
9.375	1.6	0.264	0.163	0.586	0.3151	0.972
12.5	1.6	0.226	0.163	0.494	0.3625	0.703
15.625	1.6	0.66	0.163	0.494	0.3625	0.703

4. Discussion

When persulfate salt dissociates in water, it forms persulfate anion (S₂O₈²⁻) (Eq. 6); the formed anion has a low oxidation potential and degrades organic compounds much more slowly than other oxidants at ambient temperature. Therefore, chemical or thermal activation of persulfate is necessary in order to generate sulfate free radical (SO₄^{•-}), which is a stronger oxidant (Eq. (7)) [20].



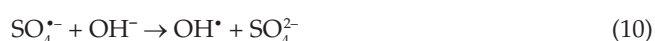
In advanced oxidation processes (AOPs) and electrochemical processes, pH of solution is the most influential parameter in system efficiency. In advanced oxidation with S₂O₈²⁻ using Fe²⁺ activation, solution pH affects either the phase of available iron and interactions of S₂O₈²⁻ with other pollutants [21]. The effects of pH on the form of iron can be demonstrated by varying pH values. Gradual increases of pH into the neutral range cause Fe²⁺ ions are more oxidized into Fe³⁺. Considering the fact that only Fe²⁺ is capable of activating S₂O₈²⁻, with decreasing Fe²⁺ to Fe³⁺ ratio, the process effectiveness significantly decreases, which is similar to that of Fenton's reagent. Also, at pH above 4, Fe²⁺ decreases and forms colloidal iron in the solution, which overall decreases the removal efficiency (Eq. (8)) [18,22].



At higher pHs (above 9), ferric-oxy hydroxyl species such as FeOH³⁺, Fe(OH)₄⁻, Fe(OH)₃[•] and Fe₂(OH)₃⁴⁺ were generated, which have slight ability to activate S₂O₈²⁻ [23]. The end product of S₂O₈²⁻ activation with Fe²⁺, resulting in SO₄^{•-}, can vary a little by pH change and leads the conditions to the production of OH[•] radical. These reactions are more common at basic pH levels (Eqs. (9) and (10)). Therefore, pH is the main factor deciding which radical to be predominant. At pH < 7, especially 3 and 5, SO₄^{•-} is the predominant radical responsible for the dye degradation (Eq. (4)). At pH between 7 and 9, both radicals are available (Eq. (9)). Under highly basic conditions, especially above 12, OH[•] radical is predominant (Eq. (10)). At basic conditions, oxidation potential of OH[•] reduced significantly. The

process efficiency decreases even in the predominance of the radical. Moreover, in comparison with OH[•], the stability of SO₄^{•-} radicals is by far more [20]. This is the reason for zero efficiency of the process at pHs 7 and 9 after 2 min.

Reaction of SO₄^{•-} and OH[•] radicals is another undesirable reaction, which takes place at high pHs and finally decreases the process efficiency due to the lack of available radicals in the oxidation system (Eq. (11)) [12,24].



Some of the reactions during the process entirely change the pH of the solutions, leading to further decrease of pH in the oxidation system. According to Eqs. (9) and (10), SO₄^{•-} has a tendency toward the generation of H⁺ and consumption of OH⁻, which, in turn, decreases pH of water environment. Moreover, H⁺ ions are generated via dissociation reactions of HSO₄⁻ in water, which consequently decrease pH more (Eqs. (12)–(14)) [23,25].



Ali khan et al. [26] in a comparative study on oxidative degradation of atrazine in aqueous solution by UV/H₂O₂/Fe²⁺, UV/S₂O₈²⁻/Fe²⁺ and UV/HSO₅⁻/Fe²⁺ concluded that the best pH value was observed in UV/HSO₅⁻/Fe²⁺ process at about 3. Also, Rao et al. [27] studied carbamazepine degradation by S₂O₈²⁻/Fe²⁺ process and reported that optimum conditions were obtained at pH about 3. They also found that the process caused pH reduction.

Romero et al. [20] studied effect of three pH values (3, 5 and 8) on Diuron abatement using activated persulfate and explained that, by pH increase, decolorization efficiency decreased and also pH decrease was observed throughout the experiments.

As iron electrode is the only source of Fe²⁺ ions used for S₂O₈²⁻ activation, amounts of released iron ions from the iron anode electrode (Eq. (15)) and regeneration of Fe²⁺ ions via continuous reduction of Fe³⁺ at the cathode surface (Eq. (16)) were controlled by current density [19,25].



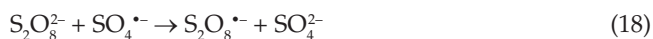
After activation of S₂O₈²⁻ with Fe²⁺ ions, oxidation occurs which forms Fe³⁺. However, due to lack of the responsible activator, a high concentration and continuous generation of Fe²⁺ is required leading to production of a large amount of iron sludge, which is a minus factor in terms of economical features. In order to solve this problem, the S₂O₈²⁻ pro-

cess was combined with the electrochemical process by using the iron electrodes. Therefore, iron is continuously generated via iron anodic electrodes and Fe^{2+} , which was oxidized to Fe^{3+} , can be regenerated by cathodic reduction reaction to Fe^{2+} ; The regeneration yields best under acidic conditions [28].

Degradation of 2,4,5-trichlorophenoxyacetic acid by a novel Electro-Fe(II)/Oxone process using iron sheet as the sacrificial anode. Wang et al. [29] introduced the Electro-Fe(II)/Oxone process by means of iron sheet as the anode, for activation of oxone, to degrade 2, 4, 5-trichlorophenoxyacetic acid. Oxone includes $2\text{KHSO}_5 \cdot \text{KHSO}_4 \cdot \text{K}_2\text{SO}_4$, where 1 mol of oxone provides 2 mol HSO_5^- , which is generated after activation of $\text{SO}_4^{\bullet-}$. Ti/RuO₂-IrO₂ was used as cathode. Further increase of Fe^{2+} from an appropriate amount does not increase the decolorization efficiency and might also lead to the production a large amounts of sludge which consequently reduces the degradation efficiency due to the competition of $\text{SO}_4^{\bullet-}$ radicals with excessive Fe^{2+} (Eq. (17)) [30,31].



Consumption of $\text{S}_2\text{O}_8^{2-}$ has a dual behavior. Increase of the oxidant concentration from an appropriate level does not increase pollutant removal and might also attract and consume $\text{SO}_4^{\bullet-}$ radicals in aqueous solution, which overallly decrease the efficiency (Eq. (18)) [32].



Therefore, 150 mg l⁻¹ was selected as the optimum concentration of $\text{S}_2\text{O}_8^{2-}$ in the present study. In most studies, in which the oxidation of organic compounds have been investigated, it was found that an increase in amount of pollutant concentration decreased removal efficiencies, which can be attributed to different reasons; first, decrement of ratios of generated radicals to the concentration of pollutant and later the generation of intermediate products which consume available radicals [19].

In most studies on oxidation of colored compounds by $\text{S}_2\text{O}_8^{2-}$ activated with iron, usually three main peaks can be seen in the adsorption spectrum of UV-Vis analysis at different time intervals under optimum conditions before reaction; these peaks are assigned to azo bonds and aromatic rings.

In Rong Xu et al. study [18], three peaks were observed in UV-Vis spectrum of Orange G structure, which were at 478, 328 and 259 nm. The peak at 259 and 328 nm were attributed to aromatic rings. Furthermore, the peak at 478 nm matched well with the characteristic of bond for azo dye. In the present study, the peak of azo bonds decreased in a higher rate in comparison with one of aromatic rings.

5. Conclusion

The results of the present study showed that the degradation rate increased with decreasing pH value. The effects of $\text{S}_2\text{O}_8^{2-}$ concentration on the degradation of AB113 can be described in two ranges. First, from 25 to 150 mg l⁻¹,

the decolorization efficiency increased. Second, from 500 to 1000 mg l⁻¹, the efficiency decreased. It was also found that the process affected the pH value of water environment during the reaction. The $\text{S}_2\text{O}_8^{2-}$ process in concert with the electrochemical process had more capability in order to generate iron electrically and persulphate activation in comparison to the separate use of each process.

Acknowledgements

The authors would like to gratefully acknowledge the financial support by the research center of Hamadan University of Medical Sciences, Iran.

References

- [1] R. Khosravi, S. Hazrati, M. Fazlzadeh, Decolorization of AR18 dye solution by electrocoagulation: sludge production and electrode loss in different current densities, *Desal. Wat. Treat.* 57 (2016) 14656–14664.
- [2] R. Khosravi, M. Fazlzadehdavil, B. Barikbin, H. Hossini, Electro-decolorization of Reactive Red 198 from aqueous solutions using aluminum electrodes systems: modeling and optimization of operating parameters, *Desal. Wat. Treat.* 54 (2015) 3152–3160.
- [3] M. Li, J.T. Li, H.W. Sun, Sonochemical decolorization of acid black 210 in the presence of exfoliated graphite. *Ultra son.* 15(1) (2008) 37–42.
- [4] M.M. Ghoneim, H.S. El-Desoky, N.M. Zidan, Electro-Fenton oxidation of Sunset Yellow FCF azo-dye in aqueous solutions. *Desalination*, 274(1) (2011) 22–30.
- [5] A.R. Rahmani, A. Shabanloo, M. Fazlzadeh, Y. Poureshgh, Investigation of operational parameters influencing in treatment of dye from water by electro-Fenton process, *Desal. Wat. Treat.* (2016) 1–8.
- [6] S.Y. Oh, S.G. Kang, D.W. Kim, P.C. Chiu, Degradation of 2,4-dinitrotoluene by persulfate activated with iron sulfides. *Chem. Eng. J.*, 172(2–3) (2011) 641–646.
- [7] S.Y. Oh, S.G. Kang, P.C. Chiu, Degradation of 2,4-dinitrotoluene by persulfate activated with zero-valent iron. *Sci. Tot. Env.*, 408(16) (2010) 3464–3468.
- [8] S. Rodriguez, A. Santos, A. Romero, F. Vicente, Kinetic of oxidation and mineralization of priority and emerging pollutants by activated persulfate. *Chem. Eng. J.*, 213 (2012) 225–234.
- [9] L. Hou, H. Zhang, X. Xue, Ultrasound enhanced heterogeneous activation of peroxydisulfate by magnetite catalyst for the degradation of tetracycline in water. *Sep. Purif. Technol.*, 84 (2012) 147–152.
- [10] A. Khataee, Application of central composite design for the optimization of photo-destruction of a textile dye using UV/ $\text{S}_2\text{O}_8^{2-}$ process. *Pol. J. Chem. Tech.*, 11(4) (2009) 38–45.
- [11] S.X. Li, W. Hu, Decolourization of Acid Chrome Blue K by Persulfate. *Pro. Env. Sci.*, 10, Part B. (0) (2011) 1078–1084.
- [12] X. Wang, L. Wang, J. Li, J. Qiu, C. Cai, H. Zhang, Degradation of Acid Orange 7 by persulfate activated with zero valent iron in the presence of ultrasonic irradiation. *Sep. Purif. Technol.*, 122 (2014) 41–46.
- [13] A. Ghauch, G. Ayoub, S. Naim, Degradation of sulfamethoxazole by persulfate assisted micrometric Fe⁰ in aqueous solution. *Chem. Eng. J.*, 228 (2013) 1168–1181.
- [14] A. Ghauch, A.M. Tuqan, Oxidation of bisoprolol in heated persulfate/ H_2O systems: Kinetics and products. *Chem. Eng. J.*, 183 (2012) 162–171.
- [15] Y.T. Lin, C. Liang, J.H. Chen Feasibility study of ultraviolet activated persulfate oxidation of phenol. *Chem.*, 82(8) (2011) 1168–1172.
- [16] L.R. Bennedson, J. Muff, E.G. Sogaard, Influence of chloride and carbonates on the reactivity of activated persulfate. *Chem.*, 86(11) (2012) 1092–1097.

- [17] H. Li, J. Wan, Y. Ma, Y. Wang, M. Huang, Influence of particle size of zero-valent iron and dissolved silica on the reactivity of activated persulfate for degradation of acid orange 7. *Chem. Eng. J.*, 237 (2014) 487–496.
- [18] X.R. Xu, X.Z. Li, Degradation of azo dye Orange G in aqueous solutions by persulfate with ferrous ion. *Sep. Purif. Technol.*, 72(1) (2010) 105–111.
- [19] J. Wu, H. Zhang, J. Qiu, Degradation of Acid Orange 7 in aqueous solution by a novel electro/Fe²⁺/peroxydisulfate process. *J. Hazard. Mater.*, 215–216(0) (2012) 138–145.
- [20] A. Romero, A. Santos, F. Vicente, C. González, Diuron abatement using activated persulphate: Effect of pH, Fe(II) and oxidant dosage. *Chem. Eng. J.*, 162(1) (2010) 257–265.
- [21] A. Rastogi, S.R. Al-Abed, D.D. Dionysiou, Sulfate radical-based ferrous–peroxymonosulfate oxidative system for PCBs degradation in aqueous and sediment systems. *Appl. Catal. B: Env.*, 85(3–4) (2009) 171–179.
- [22] N. Masomboon, C. Ratanatamskul, M.C. Lu, Chemical oxidation of 2, 6-dimethylaniline by electrochemically generated Fenton's reagent. *J. Hazard. Mater.*, 176(1–3) (2010) 92–98.
- [23] L. Zhou, W. Zheng, Y. Ji, J. Zhang, C. Zeng, Y. Zhang, et al. Ferrous-activated persulfate oxidation of arsenic(III) and diuron in aquatic system. *J. Hazard. Mater.*, 263, Part 2(0) (2013) 422–430.
- [24] H. Kusic, I. Peternel, S. Ukic, N. Koprivanac, T. Bolanca, S. Papic, et al. Modeling of iron activated persulfate oxidation treating reactive azo dye in water matrix. *Chem. Eng. J.*, 172(1) (2011) 109–121.
- [25] H. Lin, J. Wu, H. Zhang, Degradation of bisphenol A in aqueous solution by a novel electro/Fe³⁺/peroxydisulfate process. *Sep. Purif. Technol.*, 117(0) (2013) 18–23.
- [26] J.A. Khan, X. He, H.M. Khan, N.S. Shah, D.D. Dionysiou, Oxidative degradation of atrazine in aqueous solution by UV/H₂O₂/Fe²⁺, UV/Fe²⁺ and UV/Fe²⁺ processes: A comparative study. *Chem. Eng. J.*, 218 (2013) 376–383.
- [27] Y.F. Rao, L. Qu, H. Yang, W. Chu, Degradation of carbamazepine by Fe(II)-activated persulfate process. *J. Hazard. Mater.*, 268 (2014) 23–32.
- [28] H. Lin, J. Wu, H. Zhang, Degradation of clofibric acid in aqueous solution by an EC/Fe³⁺/PMS process. *Chem. Eng. J.*, 244 (2014) 514–521.
- [29] Y.R. Wang, W. Chu, Degradation of 2,4,5-trichlorophenoxyacetic acid by a novel Electro-Fe(II)/Oxone process using iron sheet as the sacrificial anode. *Wat Res.*, 45(13) (2011) 3883–3889.
- [30] S. Rodriguez, L. Vasquez, D. Costa, A. Romero, A. Santos, Oxidation of Orange G by persulfate activated by Fe(II), Fe(III) and zero valent iron (ZVI). *Chem.* 101 (2014) 86–92.
- [31] Y. Ji, C. Ferronato, A. Salvador, Y. Xi, J.M. Chovelon, Degradation of ciprofloxacin and sulfamethoxazole by ferrous-activated persulfate: Implications for remediation of groundwater contaminated by antibiotics. *Sci. Tot. Env.*, 472 (2014) 800–808.
- [32] C. Liang, Z.S. Wang, C.J. Bruell, Influence of pH on persulfate oxidation of TCE at ambient temperatures. *Chem.* 66(1) (2007) 106–113.